2021 20th International Symposium on Distributed Computing and Applications for Business Engineering and Science (DCABES)

NDT-based robot positioning system for large scale diversity environment

Qi Min[1] , Niansheng Chen[1]*, Guangyu Fan[1], Lei Rao[1]
[1]Shanghai DianJi University
Shanghai, China
hellominqi@163.com; chenns@sdju.edu.cn

Zhaohui Xu[2], Yiping Ma[2]
[2]AVIC Huadong Photoelectric Shanghai Co., Ltd.
Shanghai, China
yiping_ma@foxmail.com

***Abstract*—High accuracy positioning is an important challenge for robots in large scale environment. In order to reduce the localization errors in the environments, an efficient Normal Distributions Transform (NDT) localization method with multi-sensor fusion data fusion, namely FPCR-NDT-localization, is proposed. Firstly, the laser point cloud is pre-processed to remove the ground point cloud and the laser feature point cloud is extracted to reduce the laser point cloud alignment. Secondly, the inertial measurement unit pre-integration results are used to estimate the LIDAR inter-frame state transfer volume, and the point cloud alignment efficiency is accelerated by the feature point-based FPCR-NDT alignment method. Finally, the IMU pre-integration results and the LIDAR inter-frame alignment are fused to estimate the robot pose in the global map. In the experiments, the localization performance of HDL-localization, NDT-localization and FPCR-NDT-localization systems are tested using MulRan dataset. The results show that FPCR-NDT-localization has higher localization accuracy in different scenes and higher real-time performance compared to the original algorithm.**

Keyword—Mobile Robot; Normal Distribution Transformation; Positioning Technology; Point cloud Registration

I. INTRODUCTION

Autonomous navigation is one of the basic tasks of mobile robots[1]. In order to meet the challenges of large outdoor scene environment range and complex environmental features, it is necessary to improve the positioning accuracy and real-time performance in the process of navigation in large outdoor scenes. The positioning and navigation solutions in large scenarios mainly face the following problems. Firstly, the environment range is large and the accuracy of inter-frame pose estimation is insufficient, which leads to the accumulation of errors during the movement. Secondly, the real-time pose estimation during high-speed movement is insufficient, which leads to the decrease of positioning accuracy. Thirdly, the deflection angle of the robot is large at adjacent moments during the movement, which makes the existing inter-frame laser point cloud matching technology unable to be aligned.

II. RELATED WORK

Various solutions have been proposed to achieve localization targets and improve localization accuracy of mobile robots in large scenarios[2-5].The paper[4] proposes a positioning system based on the fusion of GNSS, LIDAR(Light Detection and Ranging), and IMU(Inertial Measurement Unit), which uses LIDAR intensity and height information to improve the accuracy and robustness of the positioning system. In this system data fusion framework Import real-time laser odometer, and use the error state Kalman filter to fuse the positioning results of different sensors. Later, the paper [5] improved the data fusion framework of [4] by introducing a factor graph optimization based approach and also adding a scene change detection component. This method makes better use of multi-sensor data, however, it relies too much on the smoothness of the sensor acquisition data.

LIDAR-based localization technology mainly realizes localization through inter-frame matching of laser point cloud data and local map matching[6-7]. During robotic LIDAR movement, point cloud matching techniques are used to determine the relative transformation relationship between two frames of the point cloud, which helps in robot odometry estimation in unknown environments[8]. Moreover, precise transformation parameters can determine the change in attitude between two moments [9]. The NDT algorithm based on the local alignment method treats the point cloud as a set of Gaussian distributions, which is applied to a statistical model of 3D points, and determines the matching parameters between the point clouds using standard optimization methods[10]. Peter et al. first used the point cloud of the current scan frame to construct a normal distribution of 2D variables for 2D data alignment[11]. Magnusson et al. applied this method to the scanning alignment process of 3D LIDAR data [12]. In large scale outdoor environment, the number of point clouds is huge and the environment is variable, so the efficiency and accuracy of point cloud alignment are reduced, to solve such problems, the feature-based laser point cloud alignment method is proposed[13]. This method of quickly aligning two frames of point clouds by features has efficient feature extraction performance and is suitable for large-scale outdoor scene feature extraction.

For application areas such as outdoor laser point cloud alignment and robot localization in large scale environment, the research of NDT matching technology based on effective point cloud feature extraction method is still meaningful. Based on the shortcomings of existing positioning systems applied to outdoor large-scale environments, the following work is made in this paper. (1) Reducing the amount of laser point cloud alignment and improving the computational efficiency by ground point filtering of the original laser point cloud.(2) Propose a Feature point cloud registration NDT algorithm, FPCR-NDT, for large-area scenes based on the original NDT method and the study of feature extraction-based LIDAR point cloud alignment.(3) Propose a lightweight multi-sensor data fusion localization system that fuses IMU and laser odometer sensor information and incorporates a local point cloud map alignment step to achieve high accuracy localization.

2473-3636/21/$31.00 ©2021 IEEE
DOI 10.1109/DCABES52998.2021.00022

III. POSITIONING SYSTEM FRAMEWORK

The corresponding schematic diagram of the positioning system is shown in Fig. 1. Firstly, in the laser point cloud pre-processing stage, non-ground point clouds are segmented to improve subsequent alignment efficiency by filtering ground point cloud information for concise processing; then, the point cloud is roughness classified and the planar feature points are extracted from it for subsequent alignment; meanwhile, the IMU odometry information is pre-integrated to predict the position transformation within two frames; in the measurement update stage, the IMU predicted position is used as the iterative initial value for the laser odometry. In the measurement update stage, the IMU predicted pose is used as the iterative initial value for the inter-frame NDT iterative alignment of the laser odometry; finally, the point cloud pose derived from the laser odometry is aligned with the local point cloud map to update the robot's own pose and achieve positioning.

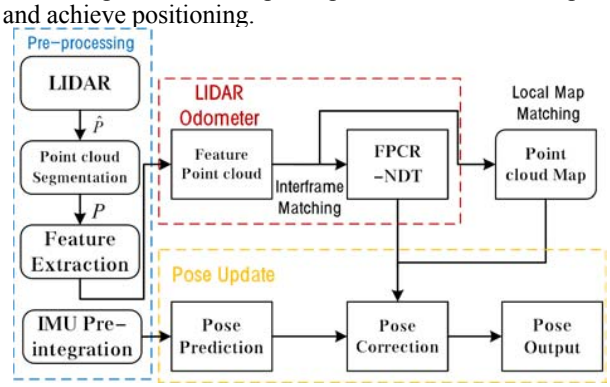

Figure 1. Schematic diagram of IMU fusion localization system based on FPCR-NDT matching algorithm

IV. 3D POINT CLOUD MAP POSITIONING SYSTEM

A. Ground Point cloud Segmentation

In the point cloud obtained by LIDAR scanning, because the ground point cloud data contains few effective features and will have certain influence on the subsequent classification and recognition of obstacles, and a large amount of redundant data on the ground will reduce the operation efficiency of the matching algorithm, so it is necessary to filter the ground part of the point cloud in the pre-processing stage of the point cloud information. In order to filter out the ground points in the point cloud, a fast ground segmentation method is used to segment the ground point cloud information. The filtered ground point cloud can effectively reduce data redundancy, reduce memory consumption.

B. Problem Description

During the robot movement, the laser odometer converts the position of the two point clouds by matching the point clouds, and the position transformation matrix of the robot during the acquisition time of the two point clouds is derived. Define the point cloud as the set $P=\{p_i \in R^3 | i=1,2\ldots,n\}$, where p_i consists of three coordinate components, $p_i=\{p_i^x, p_i^y, p_i^z\}$. In the three-dimensional space, six-dimensional vectors are defined to encode the position transformation parameter ε. Also, the robot state variable X is defined.

$$\begin{cases} \varepsilon = \left[t_x, t_y, t_z, \phi, \theta, \psi \right] \\ X = \left[x, y, z, \alpha, \beta, \gamma \right] \end{cases} \tag{1}$$

Using the Euclidean sequence z-y-x, the three-dimensional transformation function *Trans*( ) applying the transformation parameter ε is defined in (2), where the transformation parameter ε consists of the rotation parameter R and the translation parameter T.

$$Trans(\varepsilon, p) = \left[R_\phi \quad R_\theta \quad R_\psi \right] p + \begin{bmatrix} t_x \\ t_y \\ t_z \end{bmatrix} \tag{2}$$

Where R_ϕ is the rotation matrix when rotating around the x-axis at angle ϕ and $T=[t_x, t_y, t_z]^T$ is the translation vector between the origin of the two coordinate systems. In this paper, the current point cloud data to be aligned is defined as the scan frame and the completed aligned point cloud data is defined as the reference frame.

C. Feature Point Extraction

In order to improve the alignment accuracy and real-time performance, the initial point cloud is classified and features are extracted to improve the efficiency of subsequent alignment, and the schematic diagram is shown in Figure 2.

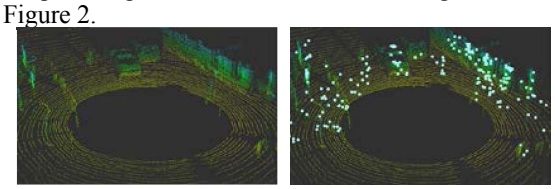

(a) Original Point Cloud (b) Feature point extraction

Figure 2. Extraction of feature points from the original point cloud

The feature points are extracted for the point cloud in Fig. (2)a using a planar feature detection based approach, so that M is taken as the point set of consecutive points x_i in the same line, where x_i is at the center of M, as shown in Fig. 3.

The roughness r of each point is calculated in (3), where $|M|$ is the number of point clouds in the set, and in this paper $|M|=15$. $X_{(k,j)}$ is the coordinates of the adjacent points to the left and right of point x_i.

$$r = \frac{1}{|M| \cdot \| X_{(k,i)}^L \|} \| \sum_{j \in M, j \neq i} (X_{(k,i)}^L - X_{(k,j)}^L) \| \tag{3}$$

Set the roughness threshold as R, traverse all x_i to consider the points with roughness less than R as feature points, as shown in Fig. (2)b.

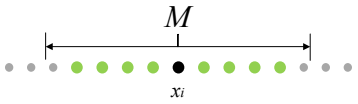

Figure 3. Single line continuous point cloud distribution

D. FPCR-NDT Point Cloud Matching Algorithm

Point cloud alignment is performed for the scanned frames and reference frames for which feature point extraction has been completed, as follows.

Step1. For the current scanned frame feature point cloud set P^S and reference frame point cloud set P^R, the feature point clouds of scanned frame and reference frame are divided into two sets of raster C^S, C^R, $P^S=\{C_1^S, C_2^S,\ldots, C_n^S\}$, $P^R=\{C_1^R, C_2^R,\ldots, C_n^R\}$,where n is the number of feature point cloud raster cells, and the feature points contained in

the raster cells generate a Gaussian distribution $N(u_i^s, \Sigma_i^s)$,$N(u_i^R, \Sigma_i^R)$.

Step2. Initialize the positional transformation parameter $\varepsilon=[t_x, t_y, t_z, \phi, \theta, \psi]$.

Step3. The alignment of the raster distribution to the inter-distribution is performed, and the inter-distribution alignment performance is judged by the following calculation results.

$$L_2 = \sqrt{\sum_{i=1}^{n}(X_i^S - X_i^R)^2} \tag{4}$$

$$\gamma_{ij} = \left[Trans(\varepsilon, u_i^S) - u_j^R \right] \tag{5}$$

The next step defines the alignment error function Ψ( ), which is used to calculate the alignment error of this parameter applied to the two-frame point cloud, as in (6).

$$\Psi(\varepsilon) = -\sum_{i=1}^{|C^S|}\sum_{j=1}^{|C^R|} \exp(-\frac{1}{2}\gamma_{ij}^T[\varepsilon_s^T \Sigma_i^R \varepsilon_s + \Sigma_j^S]^{-1}\gamma_{ij}) \tag{6}$$

Step4. The alignment error function obtained in the previous step is optimized and its gradient vector is solved by components. Let α and β be one of the components of the six-dimensional vector ε, respectively[14]. The partial derivative of this component α in ε is solved as in (7).

$$\frac{\partial}{\partial\alpha}\Psi(\varepsilon) = \frac{1}{2}(\gamma_{ij}^T B \boldsymbol{j_a} - \gamma_{ij}^T B Z_a B \gamma_{ij}) \exp(-\frac{\gamma_{ij}^T B \gamma_{ij}}{2}) \tag{7}$$

where B, $\boldsymbol{j}_\alpha$, and Z_α are the calculated process variables as shown in (8), (9), and (10).

$$B = (R^T \Sigma_i R + \Sigma_j)^{-1} \tag{8}$$

$$\boldsymbol{j_a} = \frac{\partial}{\partial\alpha}(Ru_i + t - u_j) \tag{9}$$

$$Z_a = \frac{\partial}{\partial\alpha}(R^T \Sigma_i R) \tag{10}$$

Solve the alignment error function for component β and calculate the Hessian matrix.

$$\frac{\partial^2}{\partial\alpha\partial\beta}\Psi(\varepsilon) = d_1 d_2 (\boldsymbol{j_a}^T B \boldsymbol{j_a} - 2\gamma_{ij}^T B Z_a \boldsymbol{j_a} + \gamma_{ij}^T B H_{ab} - \gamma_{ij}^T B Z_a B Z_b B \gamma_{ij} - \frac{1}{2}\gamma_{ij} B Z_{ab} B \gamma_{ij} - \frac{d_2}{4}\boldsymbol{q}^T \boldsymbol{q}) \exp(-2\frac{d_2 \gamma_{ij}^T B \gamma_{ij}}{2}) \tag{11}$$

where H_{ab}, Z_{ab}, and $\boldsymbol{q}$ are process variables as shown in (12), (13), and (14).

$$H_{ab} = \frac{\partial^2}{\partial\alpha\partial\beta}(Trans(\varepsilon, u_i^S) - u_j^R) \tag{12}$$

$$Z_{ab} = \frac{\partial^2}{\partial\alpha\partial\beta}(R^T \Sigma_i R) \tag{13}$$

$$\boldsymbol{q} = \gamma_{ij}^T B \boldsymbol{j_a} - \gamma_{ij}^T B Z_a B \gamma_{ij} \tag{14}$$

For each component α, β of the six-dimensional transformation parameter ε, the first-order derivative and second-order derivative of the error function about the components are solved, and the partial derivative expression about the variables is derived, and the alignment error function is minimized and solved, as shown in (15) and (16) to obtain the final transformation parameter ε^* of the two-frame point cloud, at which point the robot carrier state variable X_{scan} be derived as follows.

$$\varepsilon^* = \arg\min \Psi(\varepsilon) \tag{15}$$

$$X_{scan} = Trans(\varepsilon^*, X_{ref}) \tag{16}$$

E. LIDAR/IMU Combined Positioning System

The combined positioning method consists of the following steps: first, the IMU integration information is used to derive the inter-frame pose offset of the robot for coarse positioning of the robot, and this pose is imported into the FPCR-NDT matching as the initial value for the iterative alignment of the reference frame and the scan frame. After the two frames are aligned, the observed scanned frames are finely aligned with the local point cloud map, and the robot's pose in the map is obtained by using its state update. The state transfer process is defined as a discrete-time process model, and the FPCR-NDT point cloud alignment and local map matching are incorporated into the state correction process.

In the attitude prediction stage, the robot attitude information is derived from the IMU to provide initial values of the attitude, LIDAR point cloud alignment and other observation data. Set robot state $X_t = [x_t, y_t, z_t, \alpha_t, \beta_t, \gamma_t]$ at moment t during the time period in which the two state nodes (L_t, L_{t+1}) are located , the local map alignment step as a positional correction by the relative positional inferred transformation matrix T_{IMU} of IMU with the alignment relationship $T_{point2point}$ of the point cloud of the two preceding and following frames. Let the alignment relationship between the current frame and the local map be $T_{point2map}$, and derive the robot pose prediction value X'_{t+1} with the updated value X_{t+1} at moment $t+1$.

$$X'_{t+1} = T_{point2point}(T_{IMU}(X_t)) \tag{17}$$

$$X_{t+1} = T_{point2map}(X'_{t+1}) \tag{18}$$

V. EXPERIMENT AND ANALYSIS

In order to validate the localization performance of the proposed localization method, experiments are conducted to compare with existing open source solutions HDL-localization[15] with NDT-localization. In this paper, we use the mulran dataset to evaluate the localization accuracy, trajectory and other metrics of our method.

A. Experimental Settings

First, SC-LeGO-LOAM[16], an open source 3D laser slam solution with excellent performance at present, is used to generate a high-precision point cloud map. Then, the point cloud map is imported for initialization, and the robot conducts navigation experiments in this point cloud map.

Fig. 4 shows the DCC scene in the dataset. From the figure, it can be obtained that the current frame range of the point cloud is larger and can match with the local point cloud map with higher accuracy.

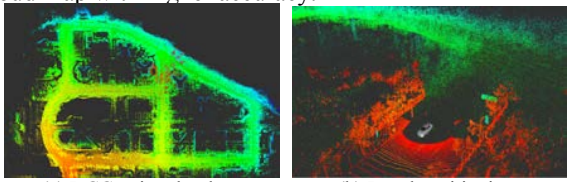

(a) DCC point cloud map (b) Local positioning

Figure 4. DCC Scene (a) shows the point cloud map of the site, and Fig. (b) shows the effect of the robot driving in the point cloud map

B. Trajectory Error Analysis

To test the performance of the FPCR-NDT positioning system, the trajectories of the above positioning system traveling in the dataset DCC scenario were derived using the trajectory evaluation tool evo, as shown in Figure 5.

From the partially enlarged area of Fig. 5, it can be concluded that among the three sets of trajectories, the trajectories of the FPCR-NDT positioning system are closer to the real motion trajectories, and most of the positioning achieves decimeter-level accuracy compared with the real trajectories, and there is no obvious cumulative error during the driving process.

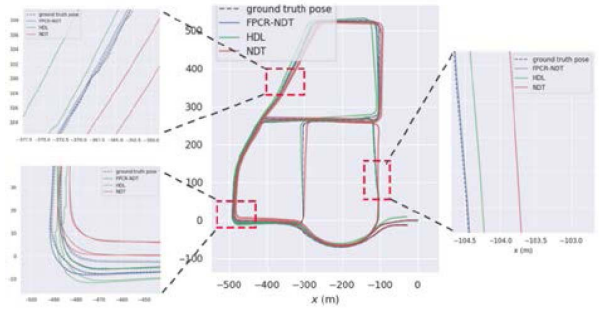

Figure 5. Comparison of three positioning methods in DCC scene motion trajectory

Figure 6 shows the comparison of the absolute positional error between the motion trajectory and the real trajectory obtained by the above three positioning systems in the DCC scenario. Table 1 shows the absolute error information for the DCC, KAIST and Riverside scenes in the Mulran dataset. In the moving process, HDL-localization and NDT-localization localization systems, which only rely on point cloud alignment for pose estimation, can hardly guarantee that the error is within a small range, and the FPCR-NDT localization system provides better pose estimation for the robot through IMU at the front end, which provides iterative initial values for subsequent alignment while ensuring computational efficiency and avoiding The iterative process falls into the local optimal situation, which is reflected in the higher accuracy and smaller root-mean-square error and standard deviation of the trajectory of the LIDAR and IMU data fusion complementary positioning method.

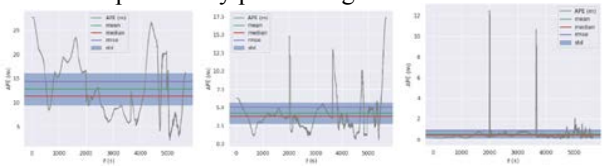

(a) NDT (b) HDL (c) FPCR-NDT

Figure 6. Absolute error of trajectory positioning of DCC scenes

VI. CONCLUSION

In order to improve the positioning accuracy for moving robots in large scale and diverse environments, a real-time localization system based on multi-sensor combination localization with feature point cloud alignment is proposed. In the system, the laser point cloud is pre-processed to remove the ground point cloud and the laser feature point cloud is extracted to reduce the laser point cloud alignment. And the inertial measurement unit pre-integration results are used to estimate the LIDAR inter-frame state transfer volume. Moreover, the LIDAR inter-frame alignment and the IMU pre-integration results are fused to estimate the robot pose in the global map. The experiments results show that FPCR-NDT-localization has higher accuracy and computing efficiency, compared to the original positioning system.

TABLE I. ABSOLUTE ERROR COMPARISON

Scene	method	mean	median	rmse	std
DCC	NDT	12.7691	11.4212	14.343	6.5164
	HDL	4.262	3.8684	5.092	2.7871
	FPCR-NDT	**0.565**	**0.4475**	**0.949**	**0.7763**
KAIST	NDT	15.195	13.6896	11.337	8.7607
	HDL	6.214	5.5518	4.366	3.7627
	FPCR-NDT	**0.832**	**0.7710**	**1.189**	**1.5937**
Riverside	NDT	16.972	16.7324	15.335	13.109
	HDL	7.185	8.6252	6.377	5.8187
	FPCR-NDT	**1.267**	**0.9018**	**1.792**	**1.8676**

REFERENCES

[1] Lambrecht, J. , and E. Funk . Edge-Enabled Autonomous Navigation and Computer Vision as a Service: A Study on Mobile Robot's Onboard Energy Consumption and Computing Requirements. 2020.

[2] Bachrach, A. G. , et al. "RANGE - robust autonomous navigation in GPS-denied environments." 2010 IEEE International Conference on Robotics and Automation IEEE, 2010.

[3] Anderson, D. M. , R. E. Estell , and T. S. Schrader . "Calculating Foraging Area Using Global Navigation Satellite System (GNSS) Technology." Rangelands 36.6(2014):31-35.

[4] Wan, G. , et al. "Robust and Precise Vehicle Localization based on Multi-sensor Fusion in Diverse City Scenes." (2017).

[5] Ding, W. , et al. "LIDAR Inertial Odometry Aided Robust LIDAR Localization System in Changing City Scenes." 2020 IEEE International Conference on Robotics and Automation (ICRA) IEEE, 2020.

[6] Wolcott, R. W. , and R. M. Eustice . "Visual localization within LIDAR maps for automated urban driving." IEEE(2014).

[7] Durrantwhyte, H. F. , and T. Bailey . "Simultaneous localization and mapping (SLAM): part II." IEEE Robotics & Amp Amp Automation Magazine 13.2(2006):99 - 110.

[8] Gressin, A. , et al. "Towards 3D LIDAR point cloud registration improvement using optimal neighborhood knowledge." ISPRS Journal of Photogrammetry and Remote Sensing 79.may(2013):240-251.

[9] Das, A. , J. Servos , and S. L. Waslander . "3D scan registration using the Normal Distributions Transform with ground segmentation and point cloud clustering." 2013 IEEE International Conference on Robotics and Automation IEEE, 2013.

[10] M Magnusson, M Magnusson, and M Magnusson. "Title: The Three-Dimensional Normal-Distributions Transform — an Efficient Representation for Registration, Surface Analysis, and." (2014).

[11] Biber, Peter . "The normal distributions transform: a new approach to laser scan matching." 2003.

[12] Magnusson, M. , A. Lilienthal , and T. Duckett . "Scan registration for autonomous mining vehicles using 3D‐NDT." Journal of Field Robotics 24.10(2007):803-827.

[13] Ji, Z. , and S. Singh . "Visual-LIDAR odometry and mapping: low-drift, robust, and fast." IEEE International Conference on Robotics & Automation IEEE, 2015.

[14] "Fast and Accurate Scan Registration through Minimization of the Distance between Compact 3D NDT Representations." International Journal of Robotics Research 31.12(2012):1377-1393.

[15] "A Portable 3D LIDAR-based System for Long-term and Wide-area People Behavior Measurement." International Journal of Advanced Robotic Systems 16.2(2019).

[16] Kim, G. , and A. Kim . "Scan Context: Egocentric Spatial Descriptor for Place Recognition Within 3D Point Cloud Map." 2018 IEEE/RSJ International Conference on Intelligent Robots and Systems (IROS) IEEE, 2018.